P-ISSN: 2304-3075; E-ISSN: 2305-4360
International Journal of Veterinary Science
www.ijvets.com; editor@ijvets.com

Research Article https://doi.org/10.47278/journal.ijvs/2024.276

Can Silver Nanoparticles Stabilized by Shilajit *(Asphaltum punjabianum)* accelerate Tibial Bone Defects Repair in Rabbits: A Preliminary Study

Madeh Sadan[1*], Rkan Almundarij[1], Mohie Haridy[2], Sabry EL-Khodery[3], Mohamed F Elzarei[4], Faten A M Abo-Aziza[5], Zarroug H Ibrahim[6] and Ahmed A H Abdellatif[7*]

[1]Department of Clinical Sciences, College of Veterinary Medicine, Qassim University, P.O. Box 6622, Buraidah, 51452, Saudi Arabia
[2]Department of Pathology and laboratory diagnosis, College of Veterinary Medicine Qassim University, P.O. Box 6622, Buraidah, 51452, Saudi Arabia
[3]Department of Internal Medicine and Infectious Diseases, Faculty of Veterinary Medicine, Mansoura University, Mansoura 35516, Egypt
[4]Animal and Poultry Production Department, College of Agriculture and Food, Qassim University, Saudi Arabia
[5]Department of Parasitology and Animal Diseases, Veterinary Research Institute, National Research Centre, Cairo 12622, Egypt
[6]Department of Medical Biosciences, College of Veterinary Medicine Qassim University, P.O. Box 6622, Buraidah, 51452, Saudi Arabia
[7]Department of Pharmaceutics, College of Pharmacy, Qassim University, P.O. Box 6622, Buraidah, 51452, Saudi Arabia
***Corresponding author:** a.abdellatif@qu.edu.sa

Article History: 24-732 Received: 21-Nov-24 Revised: 14-Dec-24 Accepted: 16-Dec-24 Online First: 29-Dec-24

ABSTRACT

Bone fractures are considered a common cause of orthopedic surgery; it can lead to serious complications on animal health. This research was designed to demonstrate the effect of silver nanoparticle (AgNPs) of Shilajit (Ag-NPS SH) on accelerating the fracture healing in a rabbit model. AgNPs were formulated through reduction with SH. The formed AgNPs-SH were characterized and identified for their size in diameter, charge and shape of the nanoformulation. Rabbits included in this study were arranged into 4 equal groups consisted of 80 adult male rabbits, creation of a bone defect (3.5mm cortical orifice) in the proximal part of right tibia of each rabbit was performed. Placebo saline, AgNPs-SH, Shilajit extract, and silver nitrate were injected at the bone defect zone in Groups 1 to 4 respectively. The bone healing process was evaluated for eight weeks; for all rabbits, postoperative anteroposterior and lateromedial radiographic views were obtained every two weeks. Precise interpretation of radiographic images was done at various times until completion of healing. The AgNPs-SH formed a pale opaque brown. Moreover, the AgNPs-SH were spherical in shape, and had absorbance of 4280nm. The diameter size of AgNPs-SH was 372.3±4.56nm and a surface charge of -23.7±1.22mV. Radiographically, the healing process was significantly ($P<0.05$) improved. A significant ($P<0.05$) increase of bone turnover biomarkers was reported in group 2 compared to other treated groups. Histopathologically, mature bone formation was reported on the 28th postoperative day in groups 2 and 3. AgNPs-SH colloidal nano-formulation could be used as a promising formulation to speed up healing process of tibial bone fracture in rabbit.

Key Words: Animals; Diagnostic Imaging; Nanoparticles; Radiography; Shilajit

INTRODUCTION

Fracture is important topic because it considered a common cause of orthopaedic surgery. It has serious effect on quality of life of both humans and animals as well as major economic and health losses. Fracture healing process is one of the important topics researched by surgeons and medical researchers. Car accidents and falling down from height were the main cause of fractures (Al-Sobayil et al. 2020; Marshall et al. 2022). Fracture healing is physiological proliferative process in which the body facilitates the repair of a bone fracture. It consists of complex processes of cell and tissue proliferation and differentiation. Many factors are affecting bone healing process including growth factors, inflammatory cytokines, antioxidants osteoclast and osteoblast cells, hormones,

Cite This Article as: Sadan M, Almundarij R, Haridy M, EL-Khodery S, Elzarei MF, Abo-Aziza FAM, Ibrahim ZH and Abdellatif AAH, 2024. Can Silver nanoparticles stabilized by Shilajit *(Asphaltum punjabianum)* accelerate tibial bone defects repair in rabbits: A preliminary study. International Journal of Veterinary Science x(x): xxxx. https://doi.org/10.47278/journal.ijvs/2024.276

amino acids and uncounted nutrients. In general, bone fracture treatment consists of pushing dislocated bone back to it places via relocation with or without anesthesia stabilizing their position and then waiting for the bones natural healing process to occur. The clinical impact of fracture is significant pain, disability, and deformity. If the fracture union is not achieved, the patient may suffer long-term disability. There are two ways to improve the fracture healing, development of implants, and improvement of bone quality to speed up and improve callus formation (Singh 2020).

Several complications of fracture such as Malunion, non-union, as well as delayed bone union are challenges that surgeons constantly face when treating fractures. Acceleration of fracture healing process is one of the important topics that surgeons are researching. There are many materials and techniques that have been used to accelerate the healing of fractures; various substances have been used in folk medicine for treatment of various bone injuries including fractures and osteoarthritis. Oral administration of Shilajit has been used to enhance and speed up the regeneration and repair of tibial bone fracture (Azizi et al. 2018; Kangari et al. 2022). Shilajit play an important role in prevention of osteoporosis through strengthening bones, improving the transfer of different minerals including, phosphate, magnesium, and calcium in the bones (AlShubaily and Jambi 2022). More than 80% of people all over the world use herbal extracts in their treatments of different diseases (Ekor 2014; Davoodi et al. 2020). Clinically and radiographic examinations as well as assaying of bone turnover biomarkers such as pyridinoline (PYD), deoxypyridinoline (DPD), bone alkaline phosphatase (BAP), Osteocalcin (OC), calcium (Ca), and phosphorus (Ph) could be used to evaluate fracture union. They considered useful tools for assessment of remodeling process in bone diseases and bone fractures (Cox et al. 2010; Sousa et al. 2015). Minimally invasive osteosynthesis (MIO) of long bone, physeal, and articular fractures as a promising fracture management modality can yield excellent outcomes when applied in carefully selected cases, performed by well experienced surgeons in the technique (Pozzi et al. 2021). Autografts are still considered the "gold standard" for fracture healing but due to limitations associated with it, new alternatives are warranted. The field of orthobiologics has provided novel approaches using scaffolds, bioactive molecules, stem cells for the treatment of bone defects. Phyto-bioactives have been widely used in alternative medicine and folklore practices for curing bone ailments. It is believed that different bioactive constituents in plants work synergistically to give the therapeutic efficacy. Bioactives in plants extracts act upon different signal transduction pathways aiding in bone healing (Singh et al. 2020). The accelerative effect of silver nanoparticles (Ag-NPS) of Shilajit on healing process of bone fractures has not been scientifically studied. Therefore, this research was carried out to detect the effect of Ag-NPS Shilajit on the speed up of fracture healing in a rabbits.

MATERIALS AND METHODS

Ethical approval

The protocol was approved by National Committee of Bioethics (NCBE) guidelines, King Abdulaziz City for Science and Technology (KACST).

Shilajit were obtained from a marketplace in Qassim, Kingdom of Saudi Arabia. Phosphate buffer (pH 7.4), NaCl, NaOH, and silver nitrate ($AgNO_3$) was obtained from Sigma Aldrich Chemie GmbH (Steinheim, Germany). All compounds were of analytical grade. The glassware was exhaustively cleaned using Millipore water and dried in an oven at 40°C overnight.

Preparation of AgNPs-SH

To prepare AgNPs-SH, in the same manner as previously mentioned (Abdellatif et al. 2022; Abdellatif et al. 2023) with some modification, 3.725g of Shilajit were added to 250mL distilled water and let it boil while stirring for 30min. The solution turned light yellow as the extract was collected, the solution was cooled and filtered. Next, 1.645g of silver nitrate solution was added to the hot Shilajit extract solution and let to stir for more 30min, the solution turned dark brown, indicating the formation of AgNPs-SH. All reactions were proceeded and performed at a boiling point of water to obtain sterile colloidal preparation. The obtained AgNPs-SH was intended to be sterile to avoid bacterial infection during the injection of AgNPs-SH, which may hinder the use of AgNPs-SH during injection into rabbits. Finally, the solution was stored in the refrigerator for further analysis and before using it in the surgical procedure.

Characterization of formulated nanoparticles AgNPs-SH

UV-VIS Spectroscopy of AgNPs-SH

The obtained formed AgNPs-SH was scanned at 300-800nm using a UV-VIS spectrophotometer (Lambda-25, Perkin Elmer, Singapore) (Aljohani et al. 2022).

Size and zeta-potential of the AgNPs-SH

AgNPs-SH were evaluated for their size distribution in terms of the standard diameters, polydispersity index (PDI) and zeta-potential using Dynamic Light Scattering (DLS) (Zetasizer-Nano, Malvern Panalytical Ltd, UK) at 25°C, in triplicate (Abdellatif and Tawfeek 2016; Abdellatif et al. 2018).

Morphology of the formulated AgNPs-SH

The morphology of the fabricated AgNPs-SH was determined using scanning electron microscope (SEM) (JOEL JFC-1300, Augsburg, Germany), and transmission electron microscope (TEM) (JEM-1230, Joel, Japan). AgNPs-SH were viewed at (10–100k) magnification power and accelerating voltage (100kV) (Abdellatif 2020; Abdellatif et al. 2021a; Abdellatif et al. 2021b; Rugaie et al. 2022).

Animals and groups

Eighty apparently healthy male New Zealand rabbits were used in this study. The ages of the rabbits were 6 to 18 months (mean 15±1.5), and their weights were 4-6kg (mean 5±0.5). Rabbits were acclimated for 1 week in suitable batteries with a temperature range of 25–29°C and a moisture content of 45–55%. They were fed artificial pellets (protein content=16%). Rabbits were vaccinated against enteric septicemia and hemorrhagic septicemia and were dewormed by subcutaneous injection of ivermectin at a dose of 0.5 ml/animal (Ivomec®, Merial Limited, Duluth, GA).

Surgical procedure

Surgery was performed with rabbits placed in lateral recumbency under general anesthesia under effect of administration of xylazine HCL 2% (5mg/kg, Bayer, Turkey), followed by ketamine HCL (25mg/kg, Zoetis, NJ, USA). Intravenous administration of prophylactic antibiotic (cefazolin, 20mg/kg, in auricular vein) was performed 30min before surgery. Following proper anesthesia of rabbits, appropriate surgical preparation of the right hindlimb of each rabbit was performed. Skin incision was performed with subsequent creation of bone defect (sized 3.5mm) in mediolateral direction at distal part of tibial tuberosity. After creation of the bone defect, it was flushed with sterile physiological saline; Groups 1 to 4 (each group, n=20) were injected at the bone defect with placebo saline, Ag-NPs nanoparticles of Shilajit, Shilajit extract, and silver nitrate respectively. Suturing of muscle and skin was performed, and preoperative administrated antibiotics were continued for 3 days post-postoperatively.

Radiographic assessment

Anterio-posterior and lateromedial radiographic views were used for evaluation of the healing of the bone defect in each operated rabbit. Radiographic assessment was performed at time 0 and every two weeks for eight weeks post-operatively using X-ray (Toshiba, Japan) with radiographic parameters of 40KV, and 0.7mAs. Precise interpretation of all obtained radiographs was done until complete healing. Modified RUS system was used for scoring of bone radiographs, scoring was graded from 1 to 4 grades according to Leow et al. (2016).

Blood Sampling and laboratory analysis

Blood samples were immediately collected from the ear vein using a 0.5-inch 29-gauge needle (Mays Company, Saudi Arabia), these samples were collected before surgery, and every two weeks until week 8 post-surgery. Directly after collection, centrifugation of blood samples was performed at 4500rpm for 20min, and obtained serums was freeze at −7°C. Measuring levels of bone alkaline phosphatase (BAP) and osteocalcin (OC) in the sera were performed using immunoassay kit by ELISA reader (BIO-TEK, INC., ELx, 800UV, USA) according to previous researches (Al-Sobayil 2008; Al-Sobayil 2010; Al-Sobayil et al. 2020). Serum calcium and phosphorus levels were assessed using kits by colorimetric method using spectrophotometric technique (Thermofisher) according to Anaraki et al. (2021). The healing process was assessed between the different experimental groups of the study.

Histopathological evaluation

Excision of the right hind leg of each rabbit was performed and the soft tissue removed. Cross sections of the bone defect area were obtained using a medium-speed saw; these sections were fixed with neutral buffered formalin 10%. For histological examination, 15% buffered formic acid solution was used to decalcify bone samples. Sections of two 5-µm-thick were prepared, stained with hematoxylin and eosin, blindly evaluated and scored by two pathologists according to the grading system (Huo et al. 1991).

Statistical analysis

The results of bone turnover biomarkers were statistically analyzed by using of commercial software (SAS version 8, SAS Institute Inc., USA). At values of $P<0.05$, findings were significant. Analysis of radiographic scores was statistically done using software (SAS 1996, SAS Institute Inc., USA). Mean±SE were evaluated. The following model was used:

$$Y_{ijk} = \mu + G_i + T_j + (G_i \times T_j) + e_{ijk}$$

Where

Y_{ijk} =Observed value for each sample

μ =Overall mean

G_i =Effect of the i^{th} treatment point (four levels; Control, Shilajit silver nanoparticle, Shilajit extract and silver nitrate)

T_j =Effect of the j^{th} time point (four levels; Week 2, 4, 6, and 8)

$G_i \times T_j$ =Effect of the interaction between treatment and time

and $\boldsymbol{e_{ijk}}$ =Random residual effects

RESULTS

Preparation and evaluation of AgNPs-SH

AgNPs were cost-effectively made using Shilajit (SH) extract. The formed AgNPs-SH was denoted by the color change to pale dark brown from yellow. The UV-VIS spectroscopy showed indication of NPs formation (Fig. 1), the formed AgNPs-SH exhibited absorbance at 480nm due to the change in surface plasmon resonance (SPR) effect. AgNPs-SH showed redshift due to the coating with Shilajit around the nucleus Ag^0. The AgNPs-SH have a size of 372.3±4.56nm (Fig. 2A) and a surface charge of -23.7±1.22mV (Fig. 2B). TEM images (Fig. 3A) showed the sphere-shaped NPs with slight clump. TEM detected a size of 250±10.68nm. Additionally, SEM image of AgNPs-FG (Fig. 3B) shows combined NPs due to the procedure of dehydrating which also recorded size about 1µm.

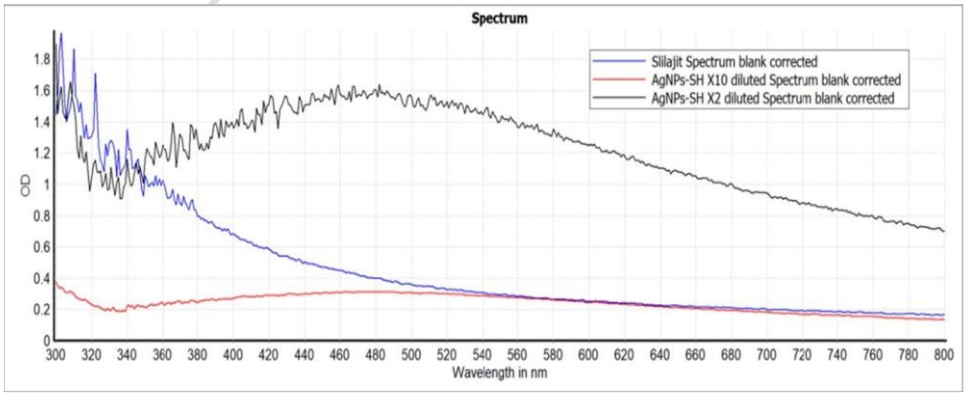

Fig. 1: The UV-VIS spectroscopy of-Shilajit extract (blue line) and the AgNPs-SH ×10 diluted (red line) and the AgNPs-SH ×2 diluted (black line) produced.

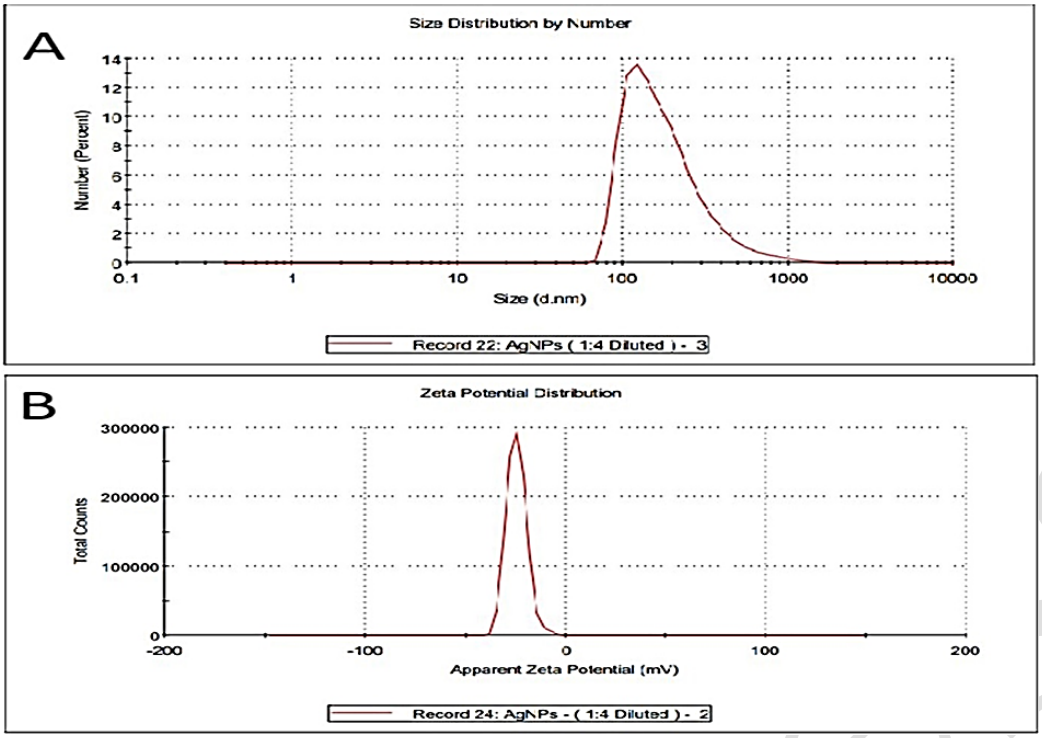

Fig. 2: Size partitioning and particle potential measurements of AgNPs-SH. (A) Particle size partitioning of AgNPs-SH. (B) ζ potential of the obtained AgNPs-SH.

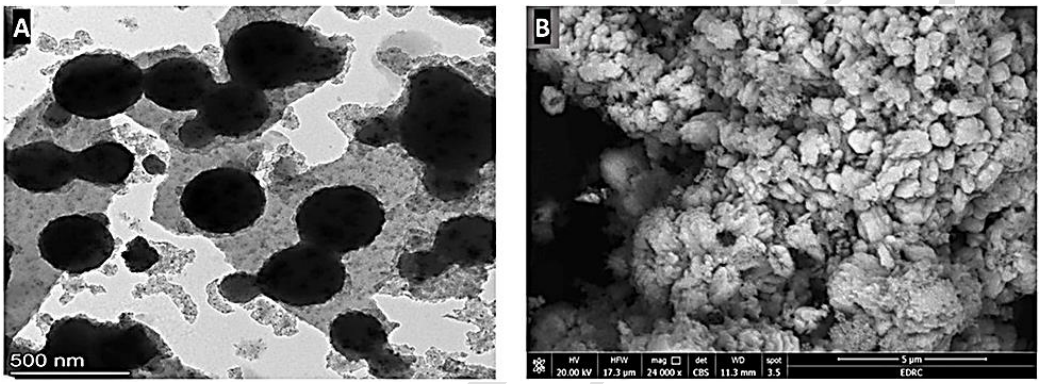

Fig. 3: (A) TEM images of AgNPs-SH, Magnification power 500000x and scale bar represented 500nm. (B) SEM image of AgNPs-FG, Magnification power 24000x & 20000 and scale bar represented 5µm.

BTMs findings

Laboratory analysis of bone turnover marker revealed significant increase ($P<0.05$) of bone Alkaline phosphatase (BAP) in treated rabbits with Ag-NPs-SH liquid (group 2) at fourth and eighth week in comparison to the other treated groups, as well as significant increase ($P<0.05$) of Osteocalcin (OC) were noticed in treated rabbits with Ag-NPs- SH liquid (group 2) from the first week to the eighth week postoperatively in comparison with other treated groups (Fig. 4). Regarding calcium and Phosphorus levels, there were mild significant differences between the treated groups.

Radiographic findings

Post-operative radiographic follow up of all studied rabbits at Zero-time revealed presence of radiolucent area at distal part of the tibial tuberosity (Fig. 5). The treatment group significantly impacts the score. The Shilajit silver nanoparticle treatment resulted in the highest mean score (4.50), significantly outperforming other treatments. The Shilajit extract group also showed a significant positive effect, with a mean score of 2.62, indicating it is more effective than the control and silver nitrate groups. The control and silver nitrate groups exhibited the lowest scores, with control being slightly higher than silver nitrate. This suggests that both the control and silver nitrate treatments had minimal or negligible effects on the measured outcome. The p-values for the group, time, and interaction effects are all highly significant ($P<0.01$), confirming that these factors have a strong and statistically reliable impact on the outcome variable. The R^2 value of 0.978 indicates that the model fits the data very well, explaining approximately 97.8% of the variability in the scores.

Practical implications

Shilajit silver nanoparticle stands out as the most effective treatment, particularly at the later time points (W8), where its effect reaches a peak. This suggests that extended exposure to this treatment leads to the most significant improvement in the measured score. The control and silver nitrate treatments were less effective, which may suggest limited therapeutic potential for these conditions under the study's experimental setup (Table 1).

Histopathological findings

Histopathological examination revealed surgical empty gap filled with granulation tissue at the bone defect at 2 weeks post-operative in groups 1 (control) and 4 (sliver nitrate) (Fig. 6a, b). In contrast, immature bone formation

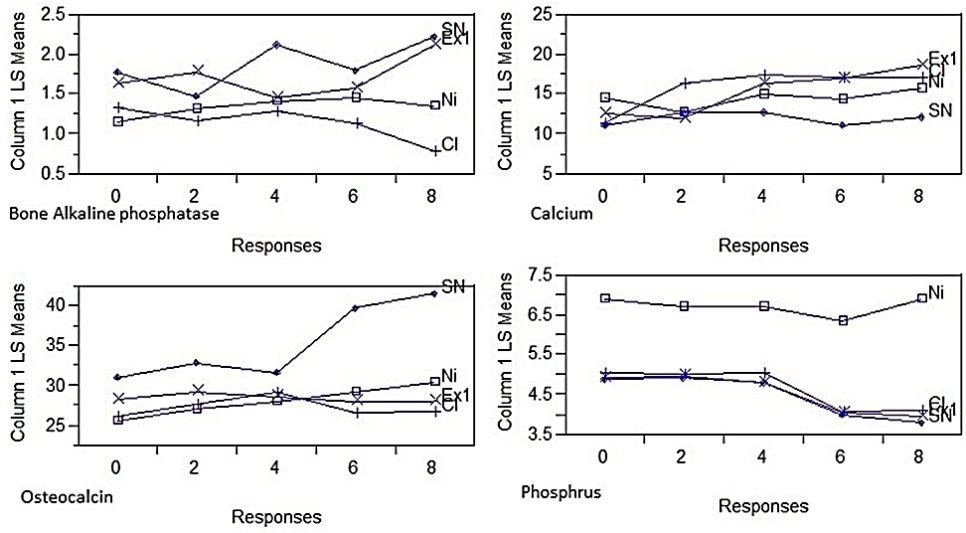

Fig. 4: (A) Bone Alkaline phosphatase (BAP), (B) Osteocalcin (OC), (C) Calcium (Ca), and (D) Phosphorus (Ph.) levels for rabbits with tibial bone treated by normal saline control group (group1), AgNPs-SH (group 2), Shilajit extract (group 3), silver nitrate (group 4). There was a significant increase in BAP, OC, Ca, and Ph levels in group 2 compared to the control group and other treated groups.

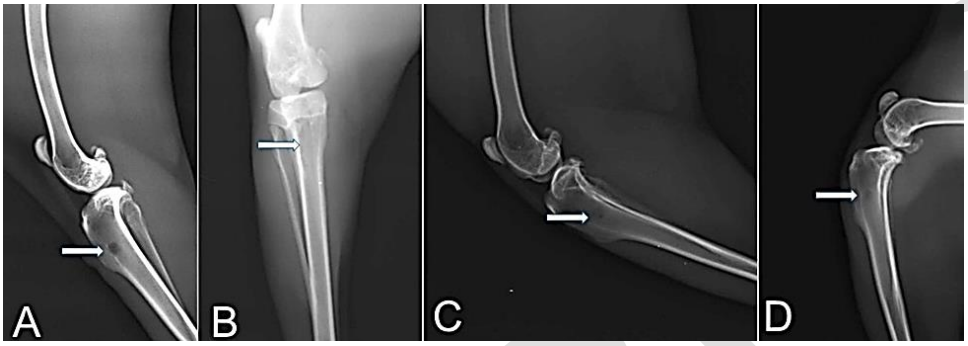

Fig. 5: Postoperative (day 56) lateral radiographs of bone defect of tibia + normal saline (A), bone defect at tibia + Shilajit silver nanoparticle (B). bone defect at tibia + Shilajit extract (C), and bone defect at tibia + silver nitrate (D). Please note complete healing of the bone defect in (B) in comparison to other studied groups.

Table 1: The interaction between time and studied treatments (least square mean ± standard error).

Treatment	Time			
	W2	W4	W6	W8
Control (Group 1)	1 ± 0.61^{d}	1.5 ± 0.43^{d}	2 ± 0.61^{cd}	1 ± 0.43^{d}
Shilajit silver nanoparticle (Group 2)	2 ± 0.61^{cd}	3 ± 0.61^{bc}	3 ± 0.61^{bc}	10 ± 0.43^{a}
Shilajit extract (Group 3)	1 ± 0.61^{d}	3 ± 0.43^{bc}	3.5 ± 0.43^{b}	3 ± 0.43^{bc}
Silver nitrate (Group 4)	1 ± 0.61^{d}	1 ± 0.43^{d}	2 ± 0.61^{cd}	2 ± 0.43^{cd}

Means differences were compared using Tukey's range test, means with the same letter in column are not significantly different (P>0.05).

(Woven cancellous bone) with cartilaginous and callous formation was observed in groups 2 (Shilajit nanoparticles) (Fig. 6c) and 3 (Shilajit extract) (Fig. 6d) at the same time. At the 4th week post-operation, mature bone with callous formation was observed in group 2 (Fig. 6e) and group 3, while immature bone formation (Woven bone) with cartilaginous and callous formation still observed in even at the 6th week post-operation in groups 1 and 4 (Fig. 6f and g). In the 8th week post-operation, mature bone formation was observed in all groups (Fig. 6j to l) except group 1 partially had also callous bone (Fig. 6i).

DISCUSSION

The field of bio-nanotechnology has introduced a new and innovative approach known as green synthesis, which offers advantages over traditional physical and chemical methods in terms of both cost and environmental impact. Additionally, the use of safe and non-toxic reagents, such as SH, further contributes to the sustainability of this process. Previous research has focused on the creation of metal nanoparticles using plant extracts, which has proven to be a secure and environmentally friendly method. It was observed that the concentrations used for AgNPs-SH were not harmful to normal cells, which is encouraging for the safety of *in vivo* studies (Mtibe et al. 2018; De Matteis et al. 2019). The smaller size of about 10nm, which is easily ionized, would release more Ag+, which is harmful to cells (Sadan et al. 2024, El-Readi et al. 2024).

The absorption wavelength signifies the increasing size, reactivity, and characterization of the nano-colloid AgNPs-SH. The UV-VIS spectra of the AgNPs-SH showed a gradual black shift and absorption peaks due to the increase in size and diameter of the nanospheroids. (Ashraf et al. 2016). In the initial nucleation stage, biogenic materials sourced from plants (SH) or other natural sources act as co-catalysts and synthesis facilitators. The shape and charges of the nano preparation colloids are changeable parameters that influence the internalization of AgNPs-SH. AgNPs-SH is considered more stable as it is coated with SH around the Ag nucleus. The interaction of electrons with the silver ion plays a crucial role in the reduction of the silver nitrate aqueous solution, leading to the formation of nano-seeds. These nano-seeds subsequently undergo stabilization through the interaction with functionalized graphene (Ekor 2014). The resulting product, AgNPs-SH, is characterized by a hydration layer and a coating of functionalized graphene, as demonstrated in equation 1.

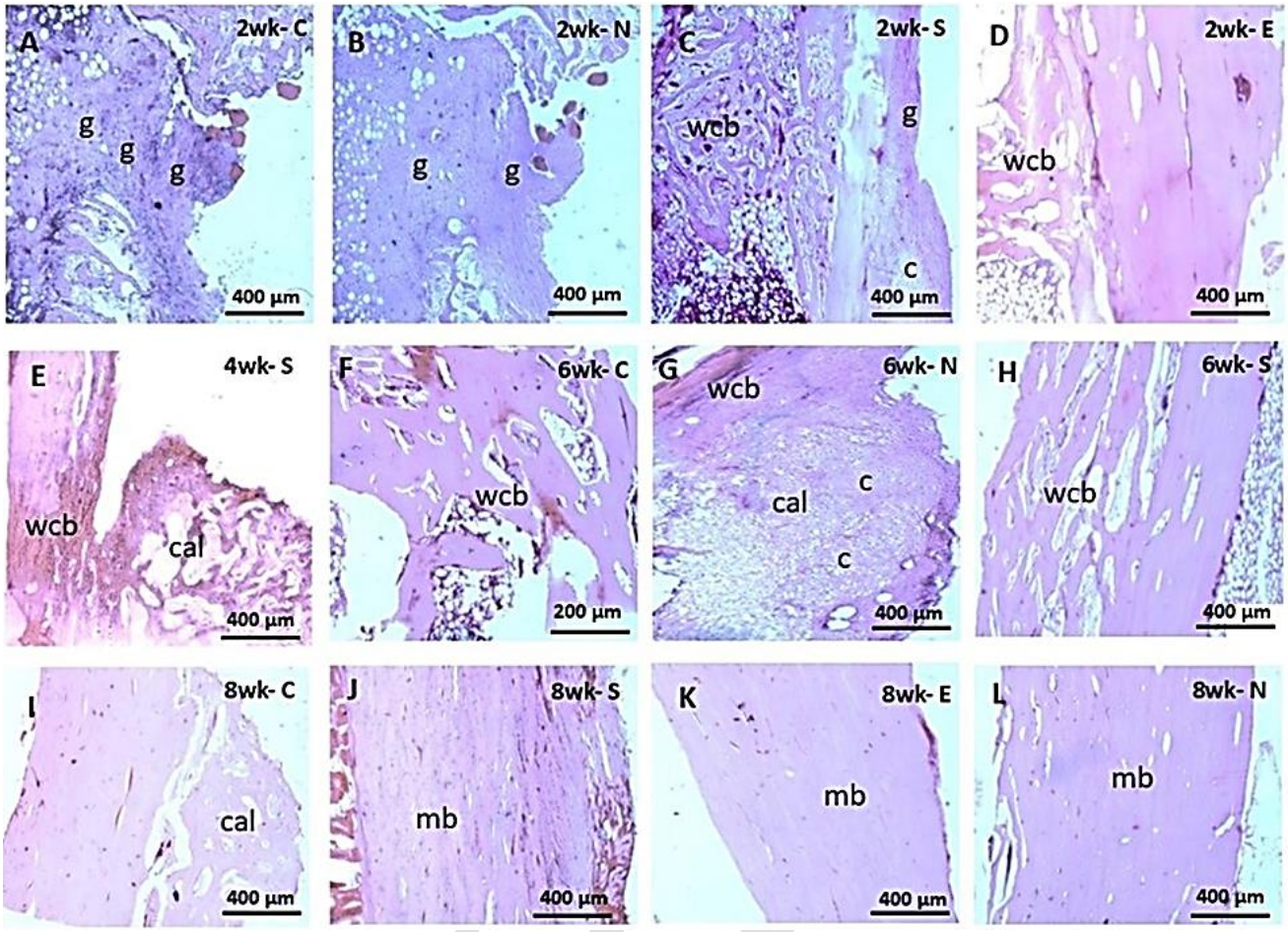

Fig. 6: Histopathological examination of the points of fracture to examine healing process in rabbits treated with placebo saline (G1), Shilajit nanoparticles (G2), Shilajit extract (G3) and silver nitrate nanoparticles (G4): Fibrous granulation (g) tissue formation was observed in the 2nd week in the control group (A) and group 4 (B), In contrast, immature bone formation (Woven cancellous bone) (wcb) with cartilaginous (c) and callous formation was observed in groups 2 (Shilajet nanoparticles) (C) and 3 (Shilajet extract) (D). At the 4th week post-operation, mature bone with callous formation (cal) was observed in groups 2, 3 (E). Immature bone formation (Woven bone) with cartilaginous and callous formation are still observed even at the 6th week post-operation in groups 1 (F) and group 4 (G). Mature bone (mb) formation was observable in the 8th week post-operation in all groups (J, K, L) except group 1 had partial also callous bone (I) (Bar=400µm, H&E).

This interaction not only contributes to the stability of the nanosilver but also imparts unique properties to the composite material (Cercado et al. 2021). They show higher zeta potential value. Barhoum et al. (2018) reported that NPs that have zeta potential higher than in the range -10 to +10mV, it is considered stable. However, those with potential zeta potential values AgNPs-SH are below -10NP which is considered highly stable without any aggregation (Abdellatif et al. 2021a).

Nucleation & Size growth=(Ag^0) + (SH) Stabilization → (Ag^+) AgNPs-SG ……> eq 1. The preparation was mixed directly with Shilajit. AgNPs-SH mixed in Shilajit is also a kind of stabilization of AgNPs-SH inside Shilajit. It should also be noted that the size obtained for AgNPs-SH was a tinier particle size as determined by TEM and DLS. The TEM determined the nucleus of AgNPs-SH resulting in smaller particles compared with that recoded by DLS (Jagadeesh et al. 2024). NPs have colorful processes in development of active and unresistant targeting. AgNPs-SH can overwhelm the limits related with standard NPs by utilizing unresistant targeting once the AgNPs-SH has been detected (Syed et al. 2020). Various mechanisms include cellular, biomechanical, hormonal, and pathological mechanisms have been involved in controlling the fracture or injury of the bone after its occurrence (Kalfas 2001). Although regeneration of fractures is physiological mechanism, different techniques have been applied to enhance the healing and regeneration of the bone fracture. Medicinal plants have been used in several researches to accelerate bone regeneration (Gorustovich et al. 2002; Adhikari et al. 2017; Eltamalawy et al. 2023). In this study the collaboration between different diagnostic techniques including RUS, BTMs and histopathological findings was used as a unique assessment tool of fracture regeneration and repair. Our finding was in accordance with El Shafaey et al. (2014) and Al-Sobayil et al. (2020). Radiological assessment following surgery (≤ 8 weeks) showed significant difference ($P<0.05$) in healing of tibial defect in rabbits treated with Ag-NPS SH (Group 2) starting from 4th week and up to 8th week compared to control group (Group 1), and at eighth week in comparison to treated rabbits with Shilajit extract (Group 3), and treated rabbits with silver nitrate (Group 4), (Table 1).

Turnover biomarkers have been used in different researches for investigation and evaluation of the bone

healing and regeneration, and it has been considered as a unique diagnostic tool for monitoring and following up of fracture repair. Measuring of bone turnover biomarkers during the healing of bone fractures and injuries could give informative evaluation of bone healing progress, and help for proper surgical decision (Al-Sobayil et al. 2020; Anaraki et al. 2021). In comparison to the other treated groups, Ag-NPS SH (group 2) had significant increase of BAP and OC. This might be contributed to BAP and OC effect on maturation of bone as reported by Vimalraj (2020), Komori (2020) and Anaraki et al. (2021).

Our findings showed, presence of fibrous tissue in group 1 and group 4 at 2nd week post operatively, while on the other hand in group 2 and group 3 immature bone (woven bone) was formed. In addition, at 4th week post operatively, mature bone formation was observed in group 2 and 3 in comparison to group 1 and group 4. This result could be contributed to incompletion of healing process and progress activity of osteoblasts in the control group (group 1) and silver nanoparticles group (group 3), while in the Ag-NPS Shilajit (group 2), healing of bone was approximately completed at 4th week. These findings were in agreement with those stated by Matos et al. (2008) and Anaraki et al. (2021).

Acknowledgments: The researcher would like to thank the Deanship of Scientific Research, Qassim University for funding the publication of this project.

Conflicts of interest: The authors declare no conflicts of interest.

Author contributions: MS, AA and RA concept and designed the proposal. MS and RA performed the experimental section. AA performed the Shilajit *(Asphaltum punjabianum)* silver nanoparticles. MH performed and evaluated the histopathological examinations. FA performed the laboratory analysis. SKH and ME analyzed the data statistically, and MS, RA, and AA analyzed and interpreted the data. All authors revised and approved the final manuscript.

Data availability: All data supporting the findings of this study are available within the manuscript and no additional data sources are required.

REFERENCES

Abdellatif AA and Tawfeek HM, 2016. Transfersomal nanoparticles for enhanced transdermal delivery of clindamycin. AAPSPharmscitech 17: 1067-1074. https://doi.org/10.1208/s12249-015-0441-7

Abdellatif AA, Alhathloul SS, Aljohani AS, Maswadeh H, Abdallah EM, Hamid Musa K and El Hamd MA, 2022. Green synthesis of silver nanoparticles incorporated aromatherapies utilized for their antioxidant and antimicrobial activities against some clinical bacterial isolates. Bioinorganic Chemistry and Applications 2022: 2432758. https://doi.org/10.1155/2022/2432758

Abdellatif AA, Alsharidah M, Al Rugaie O, Tawfeek HM and Tolba NS, 2021a. Silver nanoparticle-coated ethyl cellulose inhibits tumor necrosis factor-α of breast cancer cells. Drug Design, Development and Therapy 15: 2035-2046. https://doi.org/10.2147/DDDT.S310760

Abdellatif AA, Alturki HN and Tawfeek HM, 2021b. Different cellulosic polymers for synthesizing silver nanoparticles with antioxidant and antibacterial activities. Scientific Reports 11(1): 84. https://doi.org/10.1038/s41598-020-79834-6

Abdellatif AAH, 2020. A plausible way for excretion of metal nanoparticles via active targeting. Drug Development and Industrial Pharmacy 46(5):744-750. https://doi.org/10.1080/03639045.2020.1752710.

Abdellatif AAH, Abou-Taleb HA, Abd El Ghany AA, Lutz I and Bouazzaoui A, 2018. Targeting of somatostatin receptors expressed in blood cells using quantum dots coated with vapreotide. Saudi Pharmaceutical Journal (8): 1162-1169. https://doi.org/10.1016/j.jsps.2018.07.004

Abdellatif AAH, Alhumaydhi FA, Al Rugaie O, Tolba NS and Mousa AM, 2023. Topical silver nanoparticles reduced with ethylcellulose enhance skin wound healing. European Review for Medical and Pharmacological Sciences 27(2): 744-754. https://doi.org/10.26355/eurrev_202301_31077

Adhikari S, Gurung TM, Koirala A, Adhikari BR, Gurung R, Basnet S and Parajuli K, 2017. Study on fracture healing activity of ethnomedicinal plants in western Nepal. World Journal of Pharmaceutical Sciences 6: 93-102.

Aljohani AS, Abdellatif AA, Rasheed Z and Abdulmonem WA, 2022. Gold-nanoparticle-conjugated citrate inhibits tumor necrosis factor-α expression via suppression of nuclear factor kappa B (NF-κB) activation in breast cancer cells. Journal of Biomedical Nanotechnology 18(2): 581-588. https://doi.org/10.1166/jbn.2022.3266

AlShubaily F and Jambi E, 2022. LC/MS Profiling of Shilajit extract for antimicrobial & antifungal and cytotoxic activities. International Transaction Journal of Engineering Management, & Applied Sciences & Technologies 13: 1-13. https://doi.org/10.14456/ITJEMAST.2022.98

Al-Sobayil F, Sadan MA, El-Shafaey ES and Ahmed AF, 2020. Can bone marrow aspirate improve mandibular fracture repair in camels (Camelus dromedarius)? A preliminary study. Journal of Veterinary Science 21(6): e90. https://doi.org/10.4142/jvs.2020.21.e90

Al-Sobayil FA, 2008. Accelerative effect of fenugreek seeds on the healing of mandibular fracture in male. Research Journal of Medicinal Plant 2(2): 92-99.

Al-Sobayil FA, 2010. Circadian rhythm of bone formation biomarkers in serum of dromedary camels. Research in Veterinary Science 89(3): 455-459. https://doi.org/10.1016/j.rvsc.2010.03.024

Anaraki N, Beyraghi AH, Raisi A, Davoodi F, Farjanikish G and Sadegh AB, 2021. The effect of aqueous extract of Prunus dulcis on tibial bone healing in the rabbit. Journal of Orthopaedic Surgery and Research 16(1): 362. https://doi.org/10.1186/s13018-021-02498-z

Ashraf JM, Ansari MA, Khan H M, Alzohairy MA and Choi I, 2016. Green synthesis of silver nanoparticles and characterization of their inhibitory effects on AGEs formation using biophysical techniques. Scientific Reports 6(1): 1-10. https://doi.org/10.1038/srep20414

Azizi S, Kheirandiah R, Azari O and Torabi N, 2018. Potential pharmaceutic effect of Shilajit (mumie) on experimental osteoarthritis in rat. Comparative Clinical Pathology 27: 755-764. https://doi.org/10.1007/s00580-018-2662-0

Barhoum A, García-Betancourt ML, Rahier H and Van Assche G, 2018. Physicochemical characterization of nanomaterials: Polymorph, composition, wettability, and thermal stability. In Emerging Applications of Nanoparticles and Architecture Nanostructures 2018: 255-278. https://doi.org/10.1016/B978-0-323-51254-1.00009-9

Cercado B, Teran A, Ballesteros JC, Vázquez-Arenas J, Lara RH, Ţălu Ş and Trejo G, 2021. Nucleation and growth mechanism of Cu-Zn/AgNPs composite coatings at different concentrations of silver nanoparticles (AgNPs) in solution.

Electrochimica Acta 390: 138867. https://doi.org/10.1016/j.electacta.2021.138867

Cox G, Einhorn TA, Tzioupis C and Giannoudis PV 2010. Bone-turnover markers in fracture healing. The Journal of Bone and Joint Surgery. British Volume 92(3): 329-334. https://doi.org/10.1302/0301-620X.92B3.22787

Davoodi F, Taheri S, Raisi A, Rajabzadeh A, Ahmadvand H, Hablolvarid MH and Zakian A, 2020. Investigating the sperm parameters, oxidative stress and histopathological effects of salvia miltiorrhiza hydroalcoholic extract in the prevention of testicular ischemia reperfusion damage in rats. Theriogenology 144: 98-106. https://doi.org/10.1016/j.theriogenology.2020.01.002

De Matteis V, Rizzello L, Ingrosso C, Liatsi-Douvitsa E, De Giorgi ML, De Matteis G and Rinaldi R, 2019. Cultivar-dependent anticancer and antibacterial properties of silver nanoparticles synthesized using leaves of different Olea Europaea trees. Nanomaterials 9(11): 1544. https://doi.org/10.3390/nano9111544

Ekor M, 2014. The growing use of herbal medicines: issues relating to adverse reactions and challenges in monitoring safety. Frontiers in Pharmacology 4: 66193. https://doi.org/10.3389/fphar.2013.00177

El Shafaey EA, Aoki T, Ishii M and Yamada K, 2014. Conservative management with external coaptation technique for treatment of a severely comminuted fracture of the proximal phalanx in a Holstein-Friesian cow. Iranian Journal of Veterinary Research 15(3): 303. https://doi.org/10.22099/ijvr.2014.2545

El-Readi MZ, Abdulkarim MA, Abdellatif AA, Elzubeir ME, Refaat B, Althubiti M and Eid S Y, 2024. Doxorubicin-sanguinarine nanoparticles: formulation and evaluation of breast cancer cell apoptosis and cell cycle. Drug Development and Industrial Pharmacy. https://doi.org/10.1080/03639045.2024.2302557

Eltamalawy MM, Abdel-Aziz AF, Mohamed TM and Khedr NF, 2023. The prophylactic treatment of Egyptian, Trigonella foenum-graecum L., Extract in comparison to pure diosgenin on experimentally induced non-alcoholic steatohepatitis: New targets via AMPK, RAR, and FXR pathways. Phytomedicine Plus 3(2): 100421. https://doi.org/10.1016/j.phyplu.2023.100421

Gorustovich A, Rosenbusch M and Guglielmotti MB, 2002. Characterization of bone around titanium implants and bioactive glass particles: an experimental study in rats. International Journal of Oral Maxillofacial Implants 17(5): 644-650.

Huo MH, Troiano N W, Pelker RR, Gundberg CM and Friedlaender GE, 1991. The influence of ibuprofen on fracture repair: biomechanical, biochemical, histologic, and histomorphometric parameters in rats. Journal of Orthopaedic Research 9(3): 383-390. https://doi.org/10.1002/jor.1100090310

Jagadeesh P, Rangappa SM and Siengchin S, 2024. Advanced characterization techniques for nanostructured materials in biomedical applications. Advanced Industrial and Engineering Polymer Research 7(1): 122-143. https://doi.org/10.1016/j.aiepr.2023.03.002

Kalfas IH, 2001. Principles of bone healing. Neurosurgical Focus 10(4): 1-4. https://doi.org/10.3171/foc.2001.10.4.2

Kangari P, Roshangar L, Iraji A, Talaei-Khozani T and Razmkhah M, 2022. Accelerating effect of Shilajit on osteogenic property of adipose-derived mesenchymal stem cells (ASCs). Journal of Orthopaedic Surgery and Research 17(1): 424. https://doi.org/10.1186/s13018-022-03305-z

Komori T, 2020. What is the function of osteocalcin? Journal of Oral Biosciences 62(3): 223-227. https://doi.org/10.1016/j.job.2020.05.004

Leow JM, Clement ND, Tawonsawatruk T, Simpson CJ and Simpson AH, 2016. The radiographic union scale in tibial (RUST) fractures: Reliability of the outcome measure at an independent centre. Bone Joint Research 5 (4): 116-121. https://doi.org/10.1302/2046-3758.54.2000628

Marshall WG, Filliquist B, Tzimtzimis E, Fracka A, Miquel J, Garcia J and Fontana MD, 2022. Delayed union, non-union and mal-union in 442 dogs. Veterinary Surgery 51(7): 1087-1095. https://doi.org/10.1111/vsu.13880

Matos MA, Araújo FP and Paixão FB, 2008. Histomorphometric evaluation of bone healing in rabbit fibular osteotomy model without fixation. Journal of Orthopaedic Surgery and Research 3: 1-5. https://doi.org/10.1186/1749-799X-3-4

Mtibe A, Mokhothu T H, John MJ, Mokhena TC and Mochane MJ, 2018. Fabrication and characterization of various engineered nanomaterials. In: Handbook of Nanomaterials for Industrial Applications. Elsevier, PP: 151-171. https://doi.org/10.1016/B978-0-12-813351-4.00009-2

Pozzi A, Lewis DD, Scheuermann LM, Castelli E and Longo F, 2021. A review of minimally invasive fracture stabilization in dogs and cats. Veterinary Surgery 50 Suppl 1(Suppl 1): O5-O16. https://doi.org/10.1111/vsu.13685

Rugaie OA, Abdellatif AAH, El-Mokhtar MA, Sabet MA, Abdelfattah A, Alsharidah M, Aldubaib M, Barakat H, Abudoleh SM and Al-Regaiey KA and Tawfeek HM, 2022. Retardation of Bacterial Biofilm Formation by Coating Urinary Catheters with Metal Nanoparticle-Stabilized Polymers. Microorganisms 10(7). https://doi.org/10.3390/microorganisms10071297.

Sadan M, Naem M, Tawfeek HM, Khodier MM, Zeitoun MM, El-Khodery S and Abdellatif AA, 2024. Can silver nanoparticles stabilized by Fenugreek (Trigonella foenm-graecum) improve tibial bone defects repair in rabbits? A preliminary study. Open Veterinary Journal 14(5): 1281–1293. https://doi.org/10.5455/OVJ.2024.v14.i5.23

SAS, 1996. SAS' Procedure Guide. Version 6.12 Edition, SAS Institute, INC, Cary, NC, USA.

Singh P, Gupta A, Qayoom I, Singh S and Kumar A, 2020. Orthobiologics with phytobioactive cues: A paradigm in bone regeneration. Biomedicine and Pharmacotherapy 130: 110754. https://doi.org/10.1016/j.biopha.2020.110754

Singh V, 2020. Medicinal plants and bone healing. National Journal of Maxillofacial Surgery 11(2):309. https://doi.org/10.4103/njms.NJMS_265_20

Sousa CP, Dias IR, Lopez-Peña M, Camassa JA, Lourenço PJ, Judas FM and Reis RL, 2015. Bone turnover markers for early detection of fracture healing disturbances: A review of the scientific literature. Anais da Academia Brasileira de Ciências 87: 1049-1061. https://doi.org/10.1590/0001-3765201520150008

Syed QA, Rashid Z, Ahmad MH, Shukat R, Ishaq A, Muhammad N and Rahman HU, 2020. Nutritional and therapeutic properties of fenugreek (Trigonella foenum-graecum): a review. International Journal of Food Properties 23(1): 1777-1791. https://doi.org/10.1080/10942912.2020.1825482

Vimalraj S, 2020. Alkaline phosphatase: Structure, expression and its function in bone mineralization. Gene 754: 144855. https://doi.org/10.1016/j.gene.2020.144855